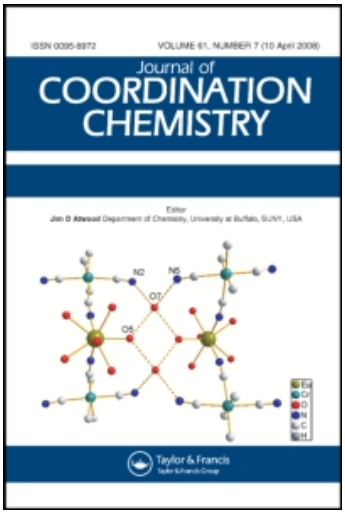

Journal of Coordination Chemistry
Publication details, including instructions for authors and subscription information:
http://www.informaworld.com/smpp/title~content=t713455674

Synthesis and characterization of a cadmium-dichloro compound of N,N,O-di-2-pyridyl ketone thiophene-2-carboxylic acid hydrazone (η^3-dpktch). The structure of [$CdCl_2$(η^3-dpktch)]

Mohammed Bakir[a]; Mark A. W. Lawrence[a]; Marvadeen Singh-Wilmot[a]
[a] Department of Chemistry, The University of the West Indies-Mona Campus, Kingston 7, Jamaica, W. I.

First published on: 18 June 2007

To cite this Article Bakir, Mohammed , Lawrence, Mark A. W. and Singh-Wilmot, Marvadeen(2007) 'Synthesis and characterization of a cadmium-dichloro compound of **N,N,O**-di-2-pyridyl ketone thiophene-2-carboxylic acid hydrazone (η^3-dpktch). The structure of [$CdCl_2$(η^3-dpktch)]', Journal of Coordination Chemistry, 60: 22, 2385 — 2399, First published on: 18 June 2007 (iFirst)
To link to this Article: DOI: 10.1080/00958970701266732
URL: http://dx.doi.org/10.1080/00958970701266732

Journal of Coordination Chemistry
Vol. 60, No. 22, 15 November 2007, 2385–2399

Taylor & Francis
Taylor & Francis Group

Synthesis and characterization of a cadmium-dichloro compound of *N*,*N*,*O*-di-2-pyridyl ketone thiophene-2-carboxylic acid hydrazone (η^3-dpktch). The structure of [$CdCl_2$(η^3-dpktch)]

MOHAMMED BAKIR*, MARK A. W. LAWRENCE
and MARVADEEN SINGH-WILMOT

Department of Chemistry, The University of the
West Indies-Mona Campus, Kingston 7, Jamaica, W. I.

(*Received 2 October 2006; in final form 24 January 2007*)

The reaction between dpktch and $CdCl_2$ in refluxing acetonitrile gave [$CdCl_2$(η^3-dpktch)] in good yield. Spectroscopic measurements divulge the coordination of dpktch and the elemental analysis confirmed its formulation. Optical measurements in *N*,*N*-dimethylformamide (dmf) and dimethylsulfoxide (DMSO) in the absence and presence of a proton donor/acceptor disclosed two highly sensitivity interlocked intra-ligand-charge-transfer transitions (ILCT) that are sensitive to their surroundings. Under basic conditions, a low-energy electronic transition with an extinction coefficient of $17{,}400 \pm 2000\ M^{-1}cm^{-1}$ appeared at ~403 nm and a peak minimum appeared at 326 nm. Under acidic conditions, a high energy electronic transition with extinction coefficient of $13{,}500 \pm 2000\ M^{-1}cm^{-1}$ appeared at ~330 nm and a shoulder appeared at ~400 nm. The addition of an acid to a dmf solution of [$CdCl_2$(η^3-dpktch)] caused the disappearance of the low energy absorption band at 403 nm and a peak maximum appeared at 330 nm. The reverse was observed when a base was added to a DMSO solution of [$CdCl_2$(η^3-dpktch)]. Electrochemical measurements reveal reduction of coordinated $CdCl_2$ and oxidation of electrodeposited cadmium metal along with ligand-based redox processes. X-ray crystallographic analysis on a monoclinic, $P2_1/n$ single crystal of [$CdCl_2$(η^3-dpktch)], confirmed the *N*,*N*,*O*-coordination of dpktch and revealed digitated units of [$CdCl_2$(η^3-dpktch)] interlocked via a web of hydrogen bonds.

Keywords: Cadmium; Di-2-pyridyl ketone; Thiophene-2-carboxylic hydrazone; X-ray; Synthesis

1. Introduction

Hydrazones and their metal compounds have been extensively studied because of their rich physical properties, reactivity patterns, and applications in many important processes that include non-linear optics, liquid crystals, medicine, electrophotographic photoreceptors, molecular sensing and catalysis [1–12]. We have been interested in the chemistry of di-2-pyridyl ketone (dpk) and its oxime and hydrazone derivatives (see scheme 1), and reported on the synthesis, characterization and structures of a variety of di-2-pyridyl ketone derivatives and their rhenium, manganese and ruthenium

*Corresponding author. Fax: 1 + 876-977-1835. Email: mohammed.bakir@uwimona.edu.jm

Journal of Coordination Chemistry
ISSN 0095-8972 print/ISSN 1029-0389 online © 2007 Taylor & Francis
DOI: 10.1080/00958970701266732

compounds [13–24]. Electrochemical measurements on *fac*-[$Re(CO)_3$(L–L)Cl] where L–L = dpk or dpkoxime revealed sequential electron transfers that led to plausible mechanisms for the electrochemical reactions of CO_2, and methylchloroformate ($ClCO_2Me$) with *fac*-[$Re(CO)_3$(dpk)Cl] and to the electrochemical reduction and oxidation of free and coordinated dpkoxime in *fac*-[$Re(CO)_3$(dpkoxime)Cl] [13–15]. Optosensing measurements on dpkhydrazones and their metal compounds exposed the existence of two interlocked intra-ligand-charge-transfer (ILCT) transitions of the donor–acceptor type that are sensitive to slight changes in their environment and allowed for the possible use of these systems as spectrophotometric sensors for a variety of substrates [16–24]. Group 12 metal ions in the concentration range 10^{-4}–10^{-9} M can be detected and determined using dpkhydrazones and their metal compounds [17, 20]. In an effort to improve the optosensing behavior of dpkhydrazones and their metal compounds, studies were initiated to explore the interactions between group 12 moieties and a variety of dpk derivatives and their metal compounds. In this report, we describe the synthesis, characterization, electrochemistry and X-ray structural analysis of the first cadmium compound of dpktch.

2. Experimental

2.1. *Reagents and reaction procedures*

Solvents were reagent grade and thoroughly deoxygenated prior to use. dpktch was prepared following a standard procedure employed for the synthesis of dpkhydrazones [16, 23, 24]. All other reagents were obtained from commercial sources and used without purification.

2.2. *Preparation of [$CdCl_2$(η^3-dpktch)]*

A mixture of $CdCl_2$ (180 mg, 0.98 mmol), dpktch (300 mg, 0.97 mmol) and acetonitrile (60 mL) was refluxed in air for 2 h. The resulting reaction mixture was reduced in volume to 20 mL and allowed to cool to room temperature. A yellow precipitate was filtered off, washed with hexane, then diethyl ether and dried; yield 27 mg (56%). Anal. Calcd for $C_{16}H_{12}CdCl_2N_4OS$ (%): C, 39.09; H, 2.46; N, 11.39%. Found: C, 39.91; H, 2.36; N, 11.02. Infrared data (KBr disk, cm^{-1}): ν(N–H) ~ 3520 broad,

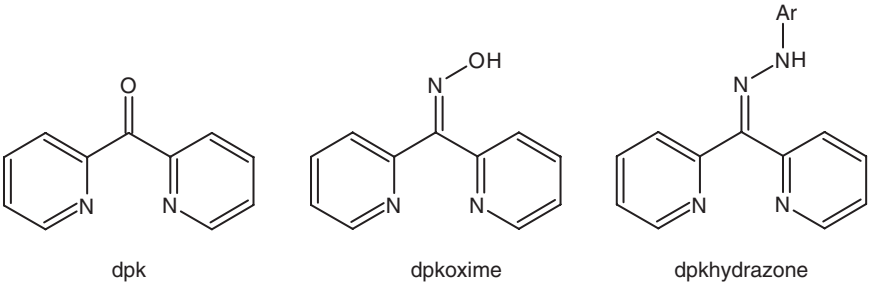

Scheme 1. Di-2-pyridyl ketone derivatives.

ν(C–H) ~ 3074, ν(C=O) 1604, ν(C=N and C=C of pyridine) 1598–1550. UV–vis {λ/nm, (ε/cm^{-1} M^{-1})}: in DMF 403 (16,900 ± 2000); in DMSO 400 (sh), 330 (13,100 ± 2000). ^{1}H NMR (δ ppm) in DMSO-d$_6$: 15.21 (s, 1H), 13.42 (s, 1H), 8.94 (b, 2 H), 8.64 (b, 2H), 8.00 (b, 10H), 7.62 (b, 2H), 7.54 (b, 4H), 7.25 (b, 2H).

2.3. *Physical measurements*

Solution ^{1}H NMR spectra were recorded on a Bruker ACE 500-MHz Fourier-transform spectrometer and referenced to the residual protons in the incompletely deuterated solvent. Infrared spectra were recorded as KBr pellets on a Perkin-Elmer Spectrum 1000 FT–IR Spectrometer. Electrochemical measurements were performed with the use of a Princeton Applied Research (PAR) Model 173 potentiostat/galvanostat and Model 276 interface, in conjunction with a digital Celebris 466 PC. Data were acquired with the EG&G PARC Headstart program and manipulated using Microsoft Excel. Measurements were performed in solutions that were 0.1 M in N(n-Bu$_4$)PF$_6$. The $E_{p,a}$, $E_{p,c}$ and $E_{1/2} = (E_{p,a} + E_{p,c})/2$ values were referenced to the quasi-silver reference electrode at room temperature and are uncorrected for junction potentials. Electrochemical cells were of conventional design based on scintillation vials or H-cells. A glassy carbon disk was used as the working electrode and a Pt wire as the counter electrode.

2.4. *X-ray crystallography*

Crystals of [CdCl$_2$(η^3-dpktch)] were obtained from a DMSO solution of [CdCl$_2$(η^3-dpktch)] when allowed to stand for several days. A single crystal was selected and mounted on a glass fiber with epoxy cement. A Bruker AXS with Mo-Kα radiation and a graphite monochromator was used for data collection and the SHELXTL software package version 5.1 was used for structure solution [25, 26]. Cell parameters and other crystallographic information are given in table 1 along with additional details concerning data collection; table 2 gives a list of atomic coordinates. All non-hydrogen atoms were refined with anisotropic thermal parameters.

2.5. *Analytical procedures*

Elemental microanalyses were performed by MEDAC Ltd., Department of Chemistry, Brunel University, Uxbridge, United Kingdom.

3. Results and discussion

Reactions of CdCl$_2$ with dpktch in refluxing acetonitrile in air gave [CdCl$_2$(η^3-dpktch)] (see scheme 2). The formulation of the isolated compound as [CdCl$_2$(η^3-dpktch)] was based on the results of its elemental analysis and a number of spectroscopic measurements, and was confirmed from the results of X-ray structural analysis done on a crystal grown from DMSO solution of [CdCl$_2$(η^3-dpktch)]. The IR spectrum of [CdCl$_2$(η^3-dpktch)] shows peaks in the ν(NH), ν(CH), ν(C=O) and the combined ν(C=C) and ν(C=N) vibrations of the pyridine (see figure 1 and experimental section) consistent with coordination of dpktch [27]. A broad band appeared in the NH stretching region, consistent with the participation of the NH group in hydrogen bonding.

Table 1. Crystal data and structure refinement for [$CdCl_2(\eta^3$-dpktch)].

Empirical formula	$C_{16}H_{12}CdCl_2N_4OS$
Formula weight	491.66
Temperature (K)	298(2)
Wavelength (Å)	0.71073
Crystal system, space group	monoclinic, $P2_1/n$
Unit cell dimensions (Å, °)	
a	9.2529(14)
b	13.3991(12)
c	14.6167(17)
α	90
β	95.462(15)
γ	90
Volume (Å^3)	1804.0(4)
Z, Calculated density (Mg m^{-3})	4, 1.810
Absorption coefficient (mm^{-1})	1.634
F(000)	968
θ range for data collection (°)	2.07–25.00
Range of h, k, l	−1/11, −15/1, −17/17
Reflections collected/unique	4144/3166 [R(int) = 0.0234]
Completeness to $\theta = 25.00$ (%)	99.7
Refinement method	Full-matrix least-squares on F^2
Data/restraints/parameters	3166/0/231
Goodness-of-fit on F^2	1.050
Final R indices [$I > 2\sigma(I)$]	$R_1 = 0.0335$, $wR_2 = 0.0854$
R indices (all data)	$R_1 = 0.0443$, $wR_2 = 0.0911$
Extinction coefficient	0.0003(3)
Largest diff. peak and hole (e Å^{-3})	1.428 and −0.354

Table 2. Atomic coordinates (×10^4) and equivalent isotropic displacement parameters (Å^2 × 10^3) for [$CdCl_2(\eta^3$-dpktch)]. U(eq) is defined as one third of the trace of the orthogonalized Uij tensor.

	x	y	z	U(eq)
Cd	421(1)	7050(1)	−667(1)	44(1)
Cl(1)	2042(1)	8396(1)	−1014(1)	58(1)
Cl(2)	−1684(1)	6892(1)	−1760(1)	58(1)
N(1)	−589(4)	7609(3)	666(2)	47(1)
N(2)	2716(4)	5552(3)	2423(2)	52(1)
N(3)	1186(3)	6090(2)	651(2)	39(1)
N(4)	2039(4)	5285(3)	514(2)	43(1)
O	1799(3)	5616(2)	−1009(2)	49(1)
S	3728(2)	4048(1)	−1592(1)	63(1)
C(11)	−1460(6)	8409(4)	649(3)	63(1)
C(12)	−1904(6)	8835(4)	1430(4)	64(1)
C(13)	−1425(5)	8434(3)	2262(4)	60(1)
C(14)	−495(5)	7617(3)	2304(3)	50(1)
C(15)	−119(4)	7210(3)	1485(3)	38(1)
C(01)	820(4)	6314(3)	1458(2)	38(1)
C(21)	3207(6)	5065(4)	3188(3)	67(1)
C(22)	2329(7)	4737(4)	3831(3)	67(1)
C(23)	881(6)	4919(4)	3691(3)	68(1)
C(24)	327(5)	5435(4)	2923(3)	55(1)
C(25)	1297(4)	5747(3)	2312(2)	39(1)
C	2351(4)	5110(3)	−360(2)	36(1)
C(31)	3359(4)	4300(3)	−491(3)	39(1)
C(32)	4146(4)	3656(3)	144(3)	45(1)
C(33)	4991(5)	3000(4)	−320(4)	65(1)
C(34)	4881(6)	3123(3)	−1239(4)	63(1)

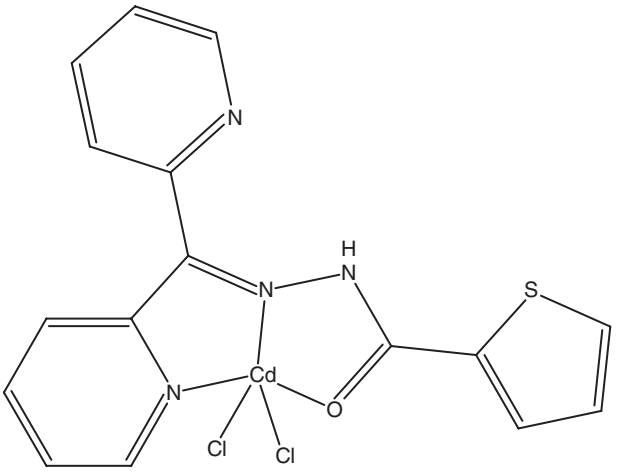

Scheme 2. [$CdCl_2(\eta^3$-dpktch)].

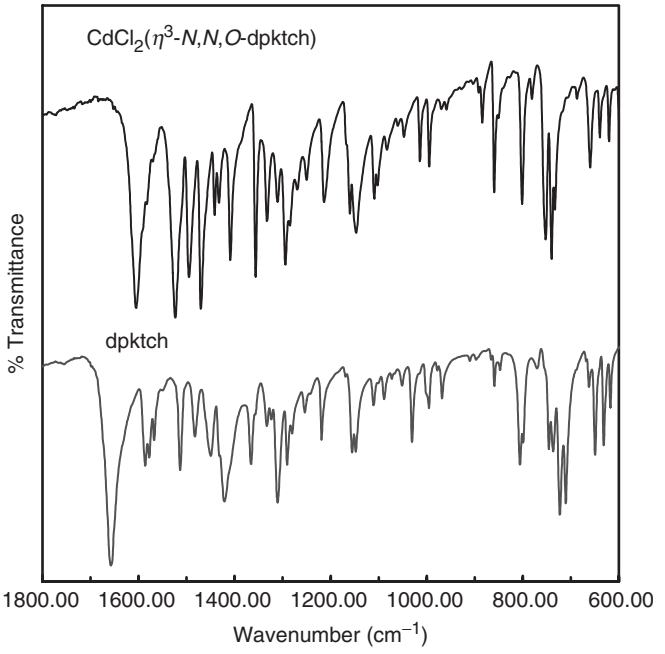

Figure 1. Infrared spectra of [$CdCl_2(\eta^3$-dpktch)] and free dpktch measured in KBr pellets.

The C–H stretching frequency appeared in the same region as in the free ligand. The amide I C=O stretching vibration of the metal compound appeared at lower frequency than the free ligand (see figure 1) pointing to coordination of the carbonyl group and a decrease in its bond order. The combined ν(C=C) and ν(C=N) of the pyridine vibrations overlap with the amide I vibration and appear in the same region as observed in the free ligand. In the amide II region between 1530–1440 cm^{-1}, the combined N–H and C–N stretching vibrations of the metal complex shift slightly to a

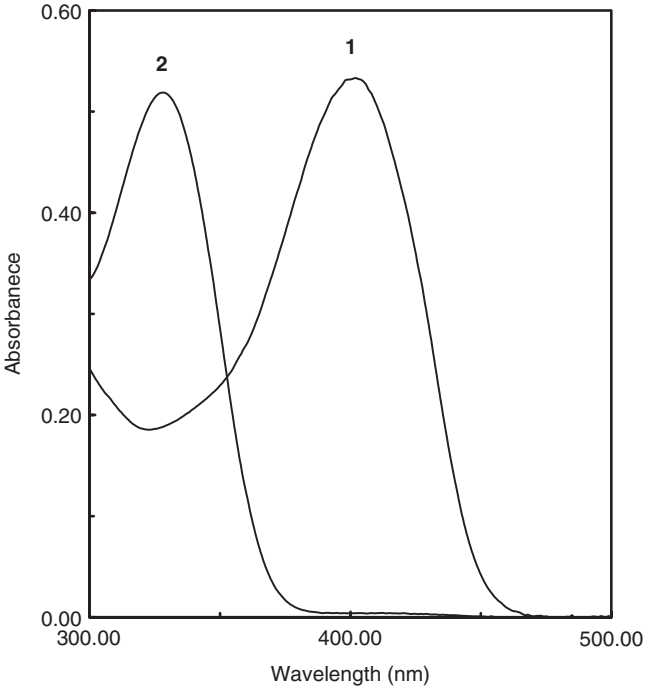

Figure 2. Electronic absorption spectra of [$CdCl_2(\eta^3$-dpktch)] measured in dmf (1) 3.00×10^{-5} M and DMSO (2) 3.20×10^{-5} M.

lower frequency and show a higher intensity than the free ligand. The N–H out-of-plane wagging of the metal complex shifts to a higher frequency than in the free ligand.

The electronic absorption spectra of [$CdCl_2(\eta^3$-dpktch)] measured between 300–500 nm in DMSO and dmf are shown in figure 2. In dmf, a highly intense absorption band appeared at 403 nm and a peak minimum appeared at 326 nm. In DMSO, a shoulder appeared at ~400 nm and a highly intense band appeared at 330 nm. These results indicate strong solvent dependence and possible solvent-complex interaction suggesting keto-enol tautomerization or acid–base inter-conversion as shown in scheme 3. This is consistent with the enhanced acidity of the amide proton upon coordination of dpktch to the metal center and is in accord with decreased acidity of dmf compared to DMSO. Under our current conditions in the concentration range 4.0×10^{-7}–4.0×10^{-5} M, a plot of the absorbance of [$CdCl_2(\eta^3$-dpktch)] *versus* its concentration in DMSO or dmf shows straight lines with slopes of $16{,}900 \pm 2000$ and $13{,}100 \pm 2000$ for the extinction coefficients of the low- and high-energy electronic states of [$CdCl_2(\eta^3$-dpktch)] in dmf and DMSO, respectively. The high values for the highly intense absorption band at 403 nm in dmf and 330 nm in DMSO hint to ILCT transitions similar to those reported for other dpkhydrazones [17, 22]. These transitions may be assigned to π–π^* of dpk followed by dpk to carbonyl charge-transfer.

The electronic absorption spectra of [$CdCl_2(\eta^3$-dpktch)] is sensitive to slight changes in its surroundings. Figure 3 shows the electronic absorption spectra of [$CdCl_2(\eta^3$-dpktch)] measured in dmf in the presence and absence of excess benzoic acid and NaOAc. When excess benzoic acid was allowed to interact with [$CdCl_2(\eta^3$-dpktch)] in dmf, the low energy absorption band observed at 403 nm in the

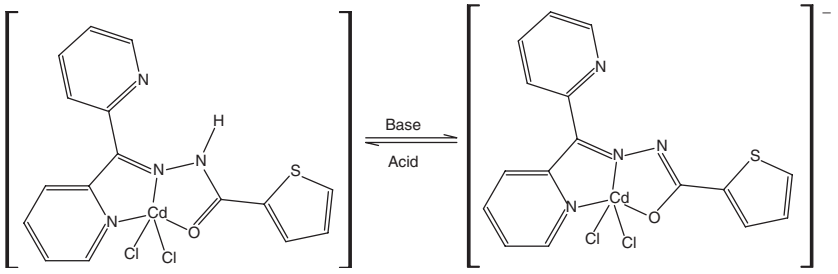

Scheme 3. Keto-enol tautomerization of $[CdCl_2(\eta^3\text{-dpktch})]$.

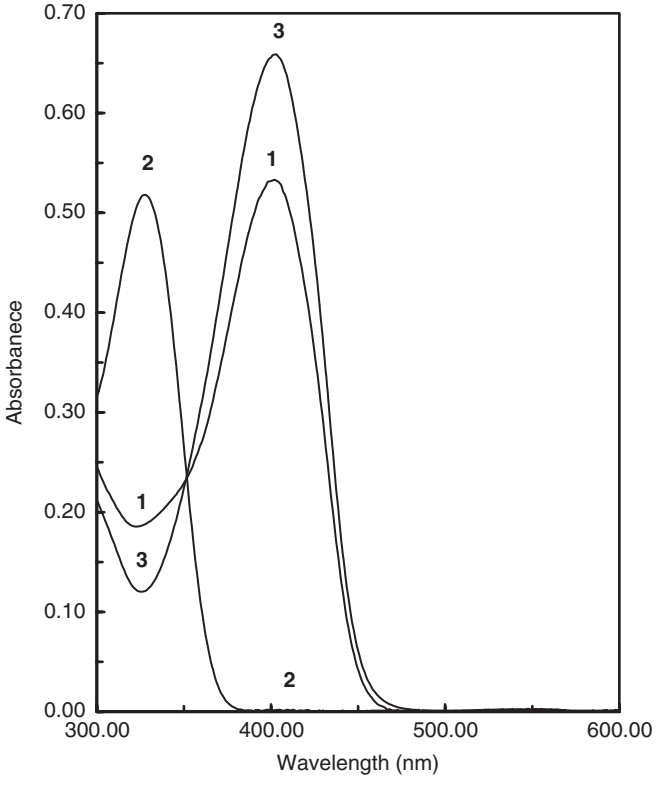

Figure 3. Electronic absorption spectra of $[CdCl_2(\eta^3\text{-dpktch})]$ 3.77×10^{-5} M in dmf (**1**), in the presence of (a) 4.30×10^{-5} M benzoic acid (**2**), and (b) 9.20×10^{-5} M sodium acetate (**3**).

absence of benzoic acid disappeared and a strong absorption band appeared at 330 nm. This led to a total conversion of the coordinated dpktch to the ketonic or acidic form and gave extension coefficients of $13{,}500 \pm 2000$ and $17{,}400 \pm 2000\ M^{-1}cm^{-1}$ for the high- and low-energy electronic states, respectively. The reverse was observed when $[CdCl_2(\eta^3\text{-dpktch})]$ was allowed to interact with excess NaOAc in dmf, or when a DMSO solution of $[CdCl_2(\eta^3\text{-N,N,O-dpktch})]$ was allowed to interact with excess NaOAc or $NaBH_4$ and gave extension coefficients of the same order as those calculated in dmf in the absence of benzoic acid and NaOAc. These results show the inter-

conversion between the high- and low-energy electronic states of [$CdCl_2(\eta^3$-dpktch)] in DMSO or dmf and the possible use of these systems (metal compound and solvent molecules) as acid/base optical sensors.

The electrochemical behavior of [$CdCl_2(\eta^3$-dpktch)] was investigated using voltammetric techniques. Cyclic voltammograms of [$CdCl_2(\eta^3$-dpktch)] measured in dmf are shown in figure 4. On a reductively-initiated scan (figure 4a), waves appeared at $E_{p,c} = -0.94$ and -1.10 V and a quasi-reversible reduction wave at $E_{1/2} = -1.50$ V ($E_{p,c} = -1.58$ and $E_{p,a} = -1.42$ V), followed by irreversible waves at $E_{p,c} = -0.80$ and -0.50 V and oxidative waves at $E_{p,a} = 1.30$, 1.50 and 1.80 V. On oxidatively-initiated scan (figure 4b), irreversible oxidations appeared at $E_{p,a} = +1.46$ and 1.78 V, followed by irreversible reductions at $E_{p,c} = -0.90$ and $E_{p,c} = -1.15$ V, quasi-reversible reduction at $E_{1/2} = 1.50$ V ($E_{p,c} = 1.52$ and $E_{p,a} = 1.48$ V), and irreversible waves at $E_{p,a} = -0.86$ and -0.53 V. In these voltammograms, the irreversible wave between $0 \rightarrow -1.20$ V can be assigned to the reduction of $CdCl_2$ and oxidation of electrodeposited cadmium metal. A cyclic voltammogram of $CdCl_2$ measured under the same conditions (figure 5f) shows irreversible waves at $E_{p,c} = -0.94$ V and $E_{p,a} = -0.76$ and -0.45 V. The appearance of an oxidative wave at $E_{p,a} = +1.30$ V upon a reductively-initiated scan hints to $2Cl^-/Cl_2$ oxidation. This is consistent with the absence of the assigned wave on an oxidatively initiated scan and is in accord with the reduction of $Cd^{2+\rightarrow 0}$ and appearance of a $Cd^{0\rightarrow 2+}$ stripping wave. The irreversible oxidations may be assigned to the ligand, as they appear in the same region as those observed for the free ligand, when measured under the same conditions (figure 5a and b).

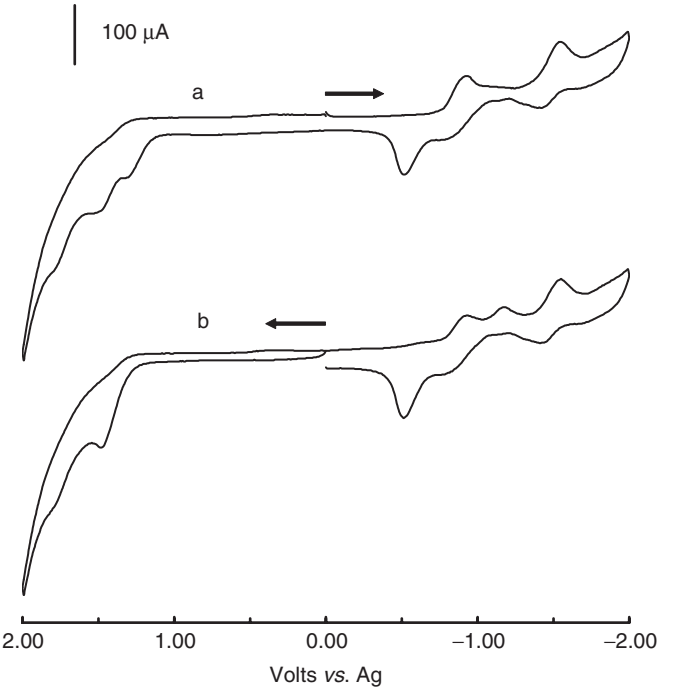

Figure 4. Cyclic voltammograms of [$CdCl_2(\eta^3$-dpktch)] measured in a dmf solution 0.1 M in [$N(n\text{-Bu})_4$]PF_6 at a glassy carbon working electrode at a scan rate of 400 mV s^{-1} *vs.* Ag.

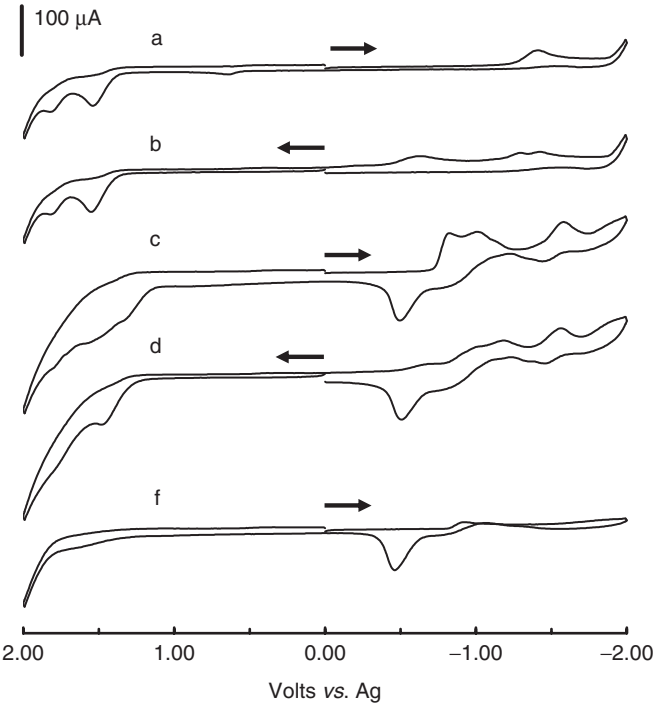

Figure 5. Cyclic voltammograms of dpktch measured in the absence (a and b) and in the presence of $CdCl_2$ (c and d) along with a cyclic voltammogram of $CdCl_2$ measured in dmf solutions 0.1 M in $[N(n\text{-}Bu)_4]PF_6$ at a glassy carbon working electrode measured at a scan rate of 400 mV s^{-1} *vs.* Ag.

The position and intensities of the waves between $0 \rightarrow -1.20$ V are scan-rate dependent. Figure 6 shows reductively-initiated scans measured on [$CdCl_2(\eta^3$-dpktch)] at different scan rates. These voltammograms show that the quasi-reversible wave between $-1.50 \rightarrow -2.00$ V retains its quasi-reversibility at different scan rates, and that the position and intensity of the waves between $0 \rightarrow -1.20$ V are scan rate dependent. As the scan rate decreases, $E_{p,c}$'s shift to more positive values and $E_{p,c}$'s becomes more pronounced while $E_{p,a}$,s remain at the same potential with $i_{p,a}^{1}/i_{p,a}^{2}$ increases. These results show the presence of two closely spaced reduction waves, due to the reduction of $Cd^{2+\rightarrow 0}$. As the scan rate decreases, the reduction of $CdCl_2$ occurs at more positive values and the resulting metal particles are oxidized at more positive potentials. The reduction of the coordinated $CdCl_2$ is scanning potential dependent. When the potential switches at more negative values, the oxidative wave ($E_{p,a}$) moves to more positive values and the associated $i_{p,a}$ increases (see figure 7).

The electrochemical reaction of dpktch with $CdCl_2$ in dmf was investigated, and figure 5 shows cyclic voltammograms of dpktch in the absence and presence of $CdCl_2$, along with a reductively initiated cyclic voltammogram of $CdCl_2$ measured under the same conditions. These voltammograms show that the addition of $CdCl_2$ to a dmf solution of dpktch gave electrochemical signature (figure 5c and d) similar to that of [$CdCl_2(\eta^3$-dpktch)] measured in dmf under the same condition except a pre-wave appeared at $E_{p,c} = -0.85$ V before the first reduction wave on a reductively initiated scan (figure 6c) of a mixture of dpktch and $CdCl_2$. The pre-wave may be due to adsorption of $CdCl_2$, dpktch, or both at the electrode surface, and is consistent with

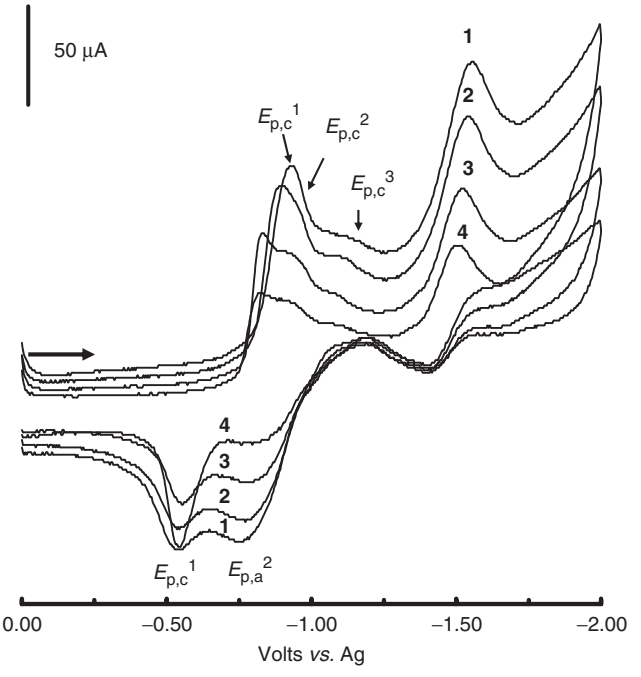

Figure 6. Cyclic voltammograms of $[CdCl_2(\eta^3\text{-dpktch})]$ measured in a dmf solution 0.1 M in $[N(n\text{-Bu})_4]PF_6$ at a glassy carbon working electrode measured at a scan rate of (1) 600, (2) 400, (3) 200 and (4) 100 mV s^{-1} *vs.* Ag.

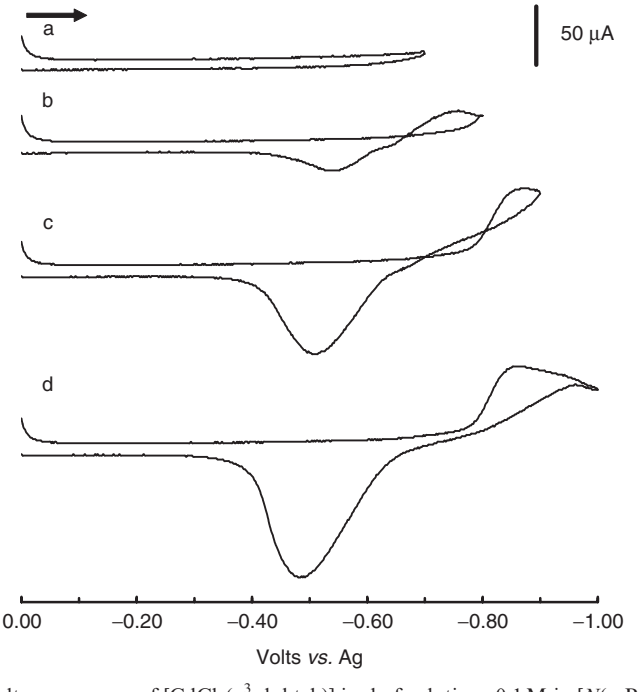

Figure 7. Cyclic voltammograms of $[CdCl_2(\eta^3\text{-dpktch})]$ in dmf solutions 0.1 M in $[N(n\text{-Bu})_4]PF_6$ at a glassy carbon working electrode at a scan rate of 200 mV s^{-1} *vs.* Ag after oxidative scan.

the disappearance of this wave upon oxidatively initiated scan (figure 6d). In the cyclic voltammogram of $CdCl_2$, waves appeared at $E_{p,c} = -0.94$ V and $E_{p,a} = -0.75$ and -0.44 V. These waves occur in the same vicinity as those observed in the voltammograms of [$CdCl_2$(η^3-dpktch)]. A mixture of dpktch and $CdCl_2$ confirm that the waves at $E_{1/2} = -0.88$ V ($E_{p,c} = -0.94$ and $E_{p,a} = -0.82$ V) and $E_{p,a} = -0.50$ V in these voltammograms are due to the reduction of coordinated $CdCl_2$ in [$CdCl_2$(η^3-dpktch)] and oxidation of electrodeposited cadmium metal.

Single crystals of [$CdCl_2$(η^3-dpktch)] grown from a DMSO solution of [$CdCl_2$(η^3-dpktch)] are in the monoclinic $P2_1/n$ space group. A view of the molecular structure of [$CdCl_2$(η^3-dpktch)] is shown in figure 8 and discloses the η^3-*N*,*N*,*O* coordination of dpktch. The coordination about cadmium is pseudo trigonal bipyramidal with two chlorine atoms and the hydrazone nitrogen atom occupying the equatorial trigonal positions. The axial positions are occupied by an oxygen atom of the hydrazone backbone and a nitrogen atom of pyridine. Deviation from trigonal-bipyramidal geometry is due to the constraints associated with the η^3-*N*,*N*,*O* coordination of dpktch to form two five-membered metallocyclic rings fused along the Cd–N3 bond. The O–Cd–N and N–Cd–N bite angles of 66 and 67° are smaller than the 90° expected for regular trigonal-bipyramidal geometry. This arrangement leaves one pyridine ring uncoordinated and exposed for potential intermolecular interactions. The bond distances and angles of the coordinated atoms (see table 3) are of the same order as the Cd–N and Cd–O bond distances of 2.4120, 2.3307 and 2.3225 Å and NCdN and NCdO bond angles of 66.67 and 66.88° reported for the only η^3-*N*,*N*,*O*-$CdCl_2$ complex, [$CdCl_2$(η^3-*N*,*N*,*O*-PICQ)], where PICQ is 2-(2′-pyridyl-3-(*N*-2-picolylimino)-4-oxo-1,2,3,4-tetrahydroquinazoline) [28].

The molecular packing pattern of [$CdCl_2$(η^3-dpktch)] is shown in figure 9 and discloses digitated units of [$CdCl_2$(η^3-dpktch)] interlocked via a web of hydrogen bonds (see figure 10 and table 4). Intramolecular interaction occurs between the amide hydrogen atom and the nitrogen atom of an uncoordinated pyridine ring to form a

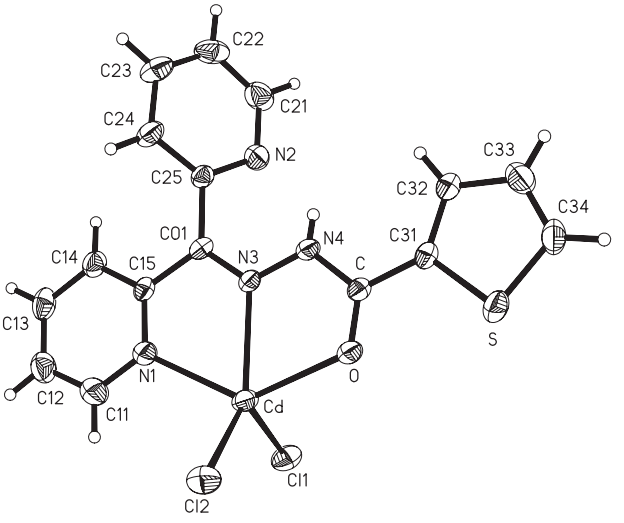

Figure 8. A view of the molecular structure of [$CdCl_2$(η^3-dpktch)]. The thermal ellipsoids are drawn at the 30% probability level.

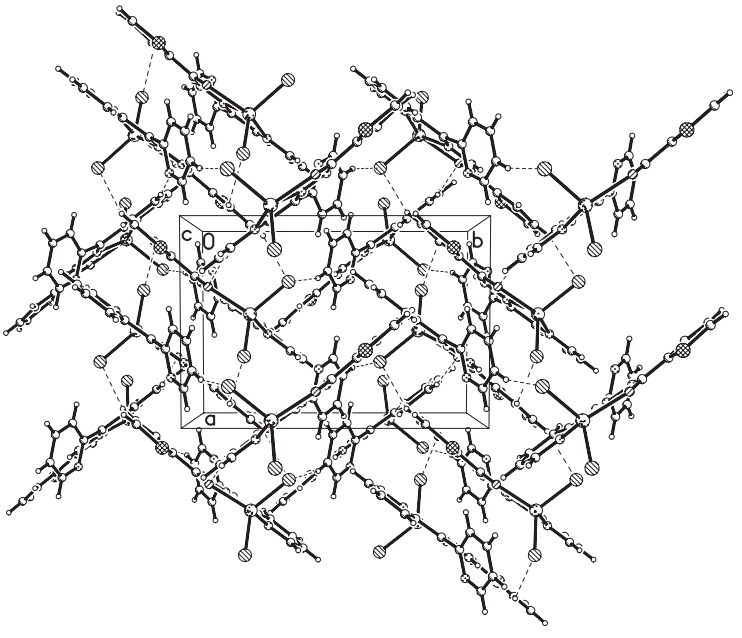

Figure 9. Packing of molecules of [$CdCl_2(\eta^3$-dpktch)]. Non-covalent bonds are represented by dashed line.

hydrogen bond of the type N–H $\cdots$ N (see figure 10). The chlorine and oxygen atoms form inter-molecular hydrogen bonds of the type C–H $\cdots$ X where X = Cl or oxygen, which interlocks all molecules in the extended structure (see figure 10). The distances and angles of the non-covalent bonds are of the same order as those reported for other compounds containing such bonds. For example, in 2-pyridinio 2-pyridyl ketone phenyl hydrazone chloride hydrate (dpkphh $\cdot$ HCl3H_2O) hydrogen bond parameters of 0.86, 2.31(6), 3.17(4) and 105(5) were reported for N–H $\cdots$ N hydrogen bonds, and parameters of 0.93, 2.44(5), 3.37(5) and 166(5) were observed for C–H $\cdots$ O hydrogen bonds [29].

Owing to their convenient synthesis, rich physical and chemical properties, potential use in non-linear optics, and molecular sensing, work is in progress by us to isolate a variety of metal compounds of polypyridyl-like ligands to explore their electro-optical properties, solid-state structures, and potential use as sensors.

4. Conclusion

The isolation of [$CdCl_2(\eta^3$-dpktch)] marks the first time a cadmium compound of dpktch has been isolated. Spectroscopic measurements disclosed the coordination of dpktch and the sensitivity of the compound to slight changes in its surroundings. Electrochemical measurements revealed sequential electronic transitions and decomposition of [$CdCl_2(\eta^3$-dpktch)]. X-ray structural analysis confirmed the identity of the isolated compound, divulged distorted trigonal bipyramidal coordination about cadmium, and showed a web of hydrogen bonds interlocking all the molecules in the extended structure.

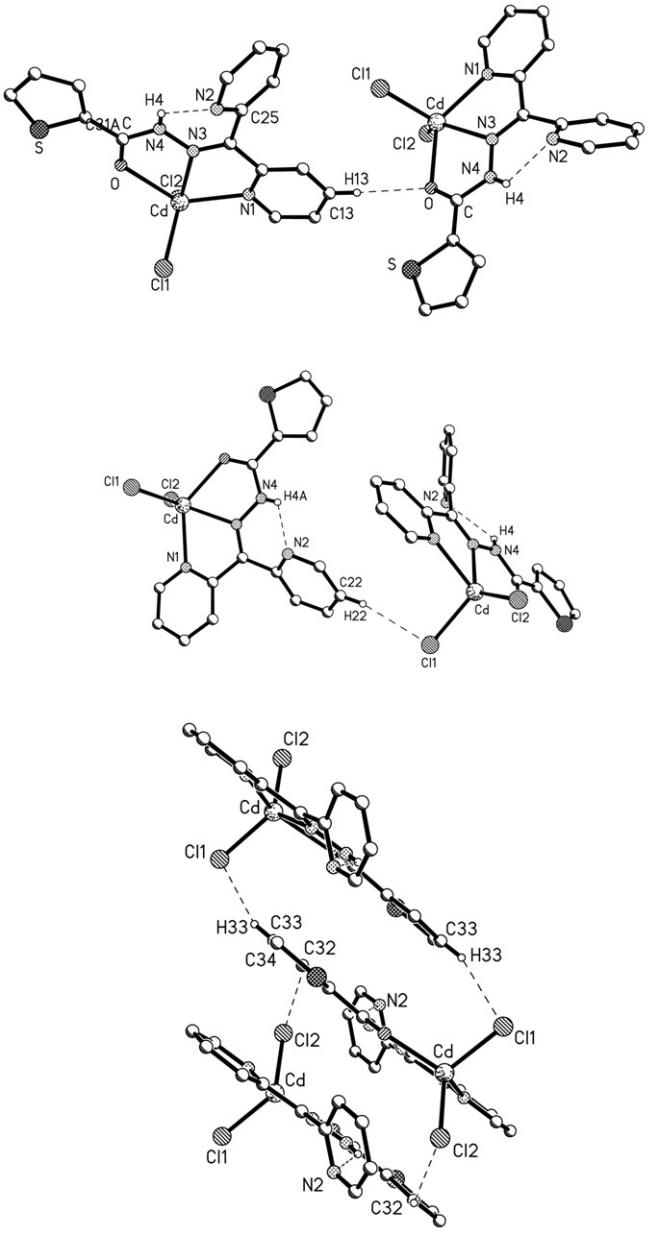

Figure 10. Views of the hydrogen bonds of $[CdCl_2(\eta^3\text{-dpktch})]$.

Supplementary material

Crystallographic data for the structure reported in this article has been deposited with the Cambridge Crystallographic Data Centre (CCDC) as supplementary material, CCDC-635074.

Table 3. Bond lengths (Å) and angles (°) for [$CdCl_2(\eta^3$-dpktch)].

Cd–N(1)	2.361(3)	Cd–N(3)	2.368(3)
Cd–O	2.385(3)	Cd–Cl(2)	2.4079(12)
Cd–Cl(1)	2.4299(12)	N(1)–C(11)	1.341(6)
N(1)–C(15)	1.345(5)	N(2)–C(25)	1.334(5)
N(2)–C(21)	1.337(6)	N(3)–C(01)	1.293(4)
N(3)–N(4)	1.362(5)	N(4)–C	1.357(5)
N(4)–H(4)	0.72(4)	O–C	1.235(4)
S–C(34)	1.684(5)	S–C(31)	1.711(4)
C(11)–C(12)	1.373(7)	C(12)–C(13)	1.365(7)
C(13)–C(14)	1.391(7)	C(15)–C(01)	1.484(5)
C(01)–C(25)	1.492(5)	C(21)–C(22)	1.372(7)
C(24)–C(25)	1.389(6)	C–C(31)	1.456(5)
C(31)–C(32)	1.416(6)	C(33)–C(34)	1.347(7)
N(1)–Cd–N(3)	67.19(11)	N(1)–Cd–O	133.61(10)
N(3)–Cd–O	66.94(9)	N(1)–Cd–Cl(2)	102.50(9)
N(3)–Cd–Cl(2)	130.69(9)	O–Cd–Cl(2)	101.82(8)
N(1)–Cd–Cl(1)	103.73(10)	N(3)–Cd–Cl(1)	115.50(9)
O–Cd–Cl(1)	101.64(8)	Cl(2)–Cd–Cl(1)	113.78(4)
C(11)–N(1)–C(15)	118.5(4)	C(11)–N(1)–Cd	121.5(3)
C(15)–N(1)–Cd	119.2(3)	C(25)–N(2)–C(21)	116.7(4)
C(01)–N(3)–N(4)	121.6(3)	C(01)–N(3)–Cd	122.1(3)
N(4)–N(3)–Cd	116.3(2)	C–N(4)–N(3)	117.0(3)
C–N(4)–H(4)	122(4)	N(3)–N(4)–H(4)	121(4)
C–O–Cd	118.2(2)	C(34)–S–C(31)	91.9(2)
N(1)–C(11)–C(12)	123.0(5)	C(13)–C(12)–C(11)	118.7(4)
C(12)–C(13)–C(14)	119.7(4)	N(1)–C(15)–C(01)	116.0(3)
C(14)–C(15)–C(01)	122.4(4)	N(3)–C(01)–C(15)	114.7(3)
N(3)–C(01)–C(25)	124.2(4)	C(15)–C(01)–C(25)	121.1(3)
N(2)–C(21)–C(22)	123.6(5)	N(2)–C(25)–C(01)	114.3(3)
C(24)–C(25)–C(01)	122.2(4)	O–C–N(4)	121.2(3)
O–C–C(31)	122.2(3)	N(4)–C–C(31)	116.7(3)
C(32)–C(31)–C	131.6(3)	C(32)–C(31)–S	111.1(3)
C–C(31)–S	117.3(3)	C(33)–C(32)–C(31)	110.0(4)
C(34)–C(33)–C(32)	114.5(4)	C(33)–C(34)–S	112.5(4)

Table 4. Hydrogen bonds for [$CdCl_2(\eta^3$–dpktch)].

D–H···A	d(D–H)	d(H···A)	d(D···A)	∠(DHA)
N(4)–H(4)···N(2)	0.72(4)	2.34(4)	2.823(5)	126(4)
N(4)–H(4)···Cl(2)^{i}	0.72(4)	2.94(5)	3.471(4)	134(5)
C(13)–H(13)···O^{ii}	0.93	2.49	3.391(5)	163.6
C(33)–H(33)···Cl(1)^{iii}	0.93	2.82	3.717(5)	161.1
C(22)–H(22)···Cl(1)^{iv}	0.93	2.76	3.659(5)	161.7
C(32)–H(32)···Cl(2)^{i}	0.93	2.87	3.512(4)	126.8

Symmetry transformations used to generate equivalent atoms: i: $-x, -y+1, -z$; ii: $x-1/2, -y+3/2, z+1/2$; iii: $-x+1, -y+1, -z$ and $-x+1/2, y-1/2, -z+1/2$.

Acknowledgments

We acknowledge Inter-America Development Bank (IDB) for the funds to establish the X-ray Laboratory at UWI-Mona.

References

[1] A. Bacchi, M. Carcelli, G. Pelizzi, C. Solinas, L. Sorace. *Inorgan. Chim. Acta*, **359**, 2275 (2006).
[2] T.B. Chaston, D.R. Richardson. *Am. J. Hematol.*, **73**, 200 (2003).
[3] R. Lygaitis, J.V. Grazulevicius, F.T. Van, C. Chevrot, V. Jankauskas, D. Jankunaite. *J. Photochem. Photobiol. A: Chem.*, **181**, 67 (2006).
[4] V.A. Milway, S.M. Tareque Abedin, L.K. Thompson, D.O. Miller. *Inorgan. Chim. Acta*, **359**, 2700 (2006).
[5] Y. Bai, D. Dang, X. Cao, C. Duan, Q. Meng. *Inorg. Chem. Commun.*, **9**, 86 (2006).
[6] V. Chandrasekhar, R. Azhakar, J.F. Bickley, A. Steiner. *Chem. Commun.*, **4**, 459 (2005).
[7] B.-D. Wang, Z.-Y. Yang, D.-W. Zhang, Y. Wang. *Spectrochim. Acta Part A*, **63**, 213 (2006).
[8] F. Chen, W. Cao, S. He, B. Wang, Y. Zhang. *Acta Phys. Chim. Sin.*, **22**(3), 280 (2006).
[9] A. Maraval, G. Magro, V. Maraval, L. Vendier, A.-M. Caminade, J.-P. Majoral. *J. Organomet. Chem.*, **691**, 1333 (2006).
[10] T. Mino, Y. Shirae, M. Sakamoto, T. Fujita. *J. Org. Chem.*, **70**, 2191 (2005).
[11] M.J. Jeong, J.H. Park, C. Lee, J.Y. Chang. *Org. Lett.*, **8**, 2221 (2006).
[12] M. Barboiu, M. Ruben, G. Blasen, N. Kyritsakas, E. Chacko, M. Dutta, O. Radekovich, K. Lenton, D.J.R. Brook, J.-M. Lehn. *Eur. J. Inorg. Chem.*, **4**, 784 (2006).
[13] M. Bakir, J.A.M. McKenzie. *Electroanal. Chem.*, **425**, 61 (1997).
[14] M. Bakir, J.A.M. McKenzie. *J. Chem. Soc.- Dalton Trans.*, 3571 (1997).
[15] M. Bakir. *J. Electroanal. Chem.*, **466**, 60 (1999).
[16] M. Bakir, K. Abdur-Rashid. *Trans. Met. Chem.*, **24**, 384 (1999).
[17] M. Bakir, K. Abdur-Rashid, W.H. Mulder. *Talanta*, **51**, 735 (2000).
[18] M. Bakir, C. Gyles. *Talanta*, **56**, 1117 (2002).
[19] M. Bakir, C. Gyles. *J. Mol. Struct.*, **753**, 35 (2005).
[20] M. Bakir, O. Green, C. Gyles. *Inorgan. Chim. Acta*, **358**, 1835 (2005).
[21] M. Bakir, O. Brown, T. Johnson. *J. Mol. Struct.*, **691**, 265 (2004).
[22] M. Bakir, K. Abdul-Rashid, C. Gyles. *Spectrochim. Acta Part A*, **59**, 2123 (2003).
[23] M. Bakir. *Eur. J. Inorg. Chem.*, **481** (2002).
[24] M. Bakir. *Inorgan. Chim. Acta*, **332**, 1 (2002).
[25] *Bruker-SHELXTL*, Software Version 5.1. Brucker AXS, Inc., Madison, Wisconsin, USA (1997).
[26] G.M. Sheldrick. *SHELX97 and SHELXL97*, University of Göttingen, Germany (1997).
[27] F.L. Boschke, W. Fresenius, J.F. K. Huber, E. Pungor, G.A. Rechnitz, W. Simon, Th.S. West (Eds). *Tables of Spectral data for Structure Determination of Organic*, Springer-Verlag, Berlin Heidelberg (1983).
[28] J.S. Casas, E.E. Castellano, M.S. Garcia-Tasende, A. Sancheza, J. Sordoa, J. Zukerman-Schpectorb. *Z. Anorg. Allg. Chem.*, **623**, 825 (1997).
[29] M. Bakir, I. Hassan, T. Johnson, O. Brown, O. Green, C. Gyles, M.D. Coley. *J. Mol. Struct.*, **688**, 213 (2004).